Effect of the nature of the polyamide on the properties and morphology of compatibilized nylon/acrylonitrile–butadiene–styrene blends

B. Majumdar*, H. Keskkula and D. R. Paul†
Department of Chemical Engineering, and Center for Polymer Research, University of Texas at Austin, Austin, TX 78712, USA
(Received 24 January 1994)

The mechanical properties and phase morphology of compatibilized blends of acrylonitrile–butadiene–styrene (ABS) with a wide range of polyamide materials having different physical and chemical characteristics were explored. The most efficient dispersion of the ABS phase and the best combination of mechanical properties occur within an optimum range of the nylon/ABS viscosity ratio. It is significantly more difficult to disperse the ABS and to generate toughened blends when the polyamide material is difunctional in character, i.e. a fraction of the chains having two amine end-groups. Increasing the inherent ductility of the polyamide leads to improved toughness of these blends.

(Keywords: nylon/ABS blend; mechanical properties; morphology)

INTRODUCTION

There has been much interest recently in combining the attractive features of incompatible polymers by interfacial reaction of added functionalized additives to form block or graft copolymer compatibilizers *in situ* during blend processing[1–23]. We have focused on the commercially interesting nylon/ABS (acrylonitrile–butadiene–styrene) system[9–15] to answer some fundamental questions related to the design of an effective compatibilization scheme[21,22]. Prior work explored the mechanical properties and morphology of nylon-6/ABS systems as a function of the miscibility and functionality characteristics of the compatibilizing polymer. The effects of rubber concentration, compatibilizer content and mixing protocol for a single polyamide matrix were also investigated. This paper examines how the physical and chemical characteristics of the polyamide phase affect the behaviour of blends compatibilized by an imidized acrylic that has proved to be very effective for this purpose.[22]

BACKGROUND

To date, two main strategies have been utilized for compatibilizing nylon/ABS blends[9–23]. One involves addition of a polymer that is miscible with the styrene–acrylonitrile (SAN) copolymer matrix of the ABS and can react with the amine end-groups of the nylon phase[15–22]. Another involves grafting of maleic anhydride to the ABS prior to blending with the polyamide[23]. Earlier work has shown that the first strategy can successfully lead to super-tough nylon/ABS blends over a broad range of compositions using imidized acrylic polymers as the compatibilizing additive[21,22].

The imidized acrylic polymers, synthesized via reactive extrusion of methylamines with poly(methyl methacrylate), generally contain at least four different types of chemical repeat structures[21,22,24–28]. This reaction scheme generates methyl glutarimide units and small amounts of methacrylic acid and glutaric anhydride units, while some methyl methacrylate units remain unchanged. By limiting the amount of acid and anhydride units through a re-esterification process[25,27], it is possible to preserve miscibility with SAN copolymers over a certain range of AN contents. An initial screening of a series of such materials[21] revealed one, see IA-250-C in *Table 2*, that is an especially effective compatibilizer, and this has been used subsequently for producing super-tough nylon-6/ABS blends over a wide range of compositions[22]. This particular imidized acrylic polymer, described in more detail later, is miscible with the SAN phase of ABS materials and contained sufficient acid functionality for reaction with the amine end-groups of the polyamide. An optimum combination of impact and tensile properties was found at roughly equal proportions of nylon-6 and ABS in blends containing 10% of this compatibilizer. As shown by transmission electron microscopy (TEM) techniques, efficient dispersion of the ABS in the polyamide phase is achieved at this composition.

TEM analysis of compatibilized blends showed that the polyamide formed the continuous phase over a broader range of compositions. This was attributed to the significantly lower melt viscosity[30–32] of the nylon-6 material relative to the ABS phase in these blends. The

*Present address: 3M, St Paul, MN 55144-1000, USA
†To whom correspondence should be addressed

0032-3861/94/25/5468-10

Table 1 Polyamides used in this study

Polymer	Commercial designation	M_n ($\times 10^3$)	End-group content (μeq g^{-1})		Relative melt viscosity[a]	Izod impact (J m^{-1})	Modulus (GPa)	Yield stress (MPa)	Elongation at break (%)	Source
			NH_2	COOH						
Nylon-6	Capron 8202	17	59.1	60.8	0.5	42	2.7	70	110	Allied-Signal Inc.
Nylon-6	Capron 8207F	22	47.9	43.0	1.0	40	2.8	70	233	Allied-Signal Inc.
Nylon-6	Capron 8209	31	34.8	28.8	2.1	50	2.7	71	143	Allied-Signal Inc.
Nylon-6	B5	37	28.1	23.8	3.3	55	2.9	73	75	BASF
Nylon-6	XPN 1250	18	73.0	17.2	0.8	52	2.7	70	46	Allied-Signal Inc.
Nylon-6,6	Zytel 101	17	46.0	n.a.	1.1[b]	45	2.7	80	210	E.I. du Pont Co.
Nylon-6/Nylon-6,6 (65/15) copolymer	XPN 1539F	22	52.7	50.1	1.1	58	2.1	63	121	Allied-Signal Inc.
Nylon-6/Nylon-6,6 (16/84) copolymer	Vydyne 86X	n.a.[c]	49.0	n.a.	1.0	46	2.3	67	80	Monsanto Chemical Co.
Nylon-6,10	Nylon-6,10	25	32.6	n.a.	1.4[b]	62	n.t.[d]	n.t.	n.t.	Aldrich Chemical Co.
Nylon-6,12	Zytel 158 L	n.a.	43.8	41.7	1.8	81	1.9	52	240	E.I. du Pont Co.
Nylon-11	BMNO TL	25	46.4	43.4	0.4	72	1.2	41	250	Atochem Inc.
Nylon-11	BESNO TL	n.a.	n.a.	n.a.	1.3	68	1.2	n.t.	n.t.	Atochem Inc.
Nylon-11	BESVO	n.a.	n.a.	n.a.	3.3	n.t.	n.t.	n.t.	n.t.	Atochem Inc.
Nylon-11	BESHVO	n.a.	n.a.	n.a.	3.9	70	1.2	n.t.	n.t.	Atochem Inc.
Nylon-12,12	Zytel 40-401	n.a.	46.0	47.6	1.5	220	1.6	45	400	E.I. du Pont Co.

[a] Brabender torque at 240°C and 60 rev min^{-1} after 10 min divided by that of Capron 8207F nylon-6
[b] Same as *a*, except at 280°C
[c] n.a. = not available
[d] n.t. = not tested

ABS material shows a strong shear-thinning behaviour while the nylon-6 was found to be more Newtonian[22].

Other work from this laboratory on toughening of polyamide blends with maleated, elastomeric triblock copolymers (ethylene/butylene mid-block and styrene end-blocks, or SEBS-*g*-MA) revealed a strong effect of the chemical characteristics of the nylon matrix on the morphology of the rubber phase for blends prepared in a single-screw extruder[33-35]. Monofunctional polyamides (nylon-*x*) that have only one amine end-group per molecule lead to very small, regular rubber particles, ~0.05 μm in size. Difunctional polyamides (nylon-*x*,*y*), on the other hand, lead to much larger, complex-shaped particles owing to the two-point grafting to rubber particles that is possible when the polyamide has some chains with two amine end-groups. The rubber particle size and the ductile–brittle transition temperature of these blends depend on the methylene content (CH_2/NHCO) in the repeat units of difunctional polyamides[35]. The chemical functionality of the polyamide matrix also affects the morphology of the dispersed phase in model nylon/SAN systems compatibilized with imidized acrylic polymers. In general, introduction of difunctional reactivity in the polyamide via either copolymerization or end-capping that leads to excess amine end-groups generates larger and increasingly complex dispersed particles.

EXPERIMENTAL

Table 1 summarizes pertinent information about the various polyamides used in this work. Five different nylon-6 materials including the Capron 8207F used earlier are employed here. For four of these, the amine and the carboxyl end-groups are closely matched, while the XPN 1250 material has a significantly greater number of amine than carboxylic end-groups (see *Table 1*). The end-group concentrations were determined by titration techniques[36]. Some of the polyamides in *Table 1* have difunctional character, i.e. some of the chains have two amine end-groups, viz. nylon-6-6, nylon-6/nylon-6,6 copolymers, nylon-6,10, nylon-6-12 and nylon-12,12. The series of nylon-11 materials with different molecular weights shown in *Table 1* are also used here.

The ABS material, designated as BL-65 from Sumitomo Naugatuk Co., is the same as used in previous work[19,37,38]. This material consists of SAN copolymer grafted to a butadiene-based latex rubber that has a broad distribution of particle sizes with typical particle diameters in the 0.2 μm range. The SAN phase contains 24% AN by weight and 40% is grafted to the rubber. The total rubber content of this material is 50%. The imidized acrylic material, IA-250-C, contains 2.18% free acid and 1.08% anhydride, and 55.7% by weight glutarimide units. The remaining units in this polymer are methyl methacrylate groups. This material is miscible with the SAN matrix of the ABS polymer employed here[21,22].

For rheological characterization, the various polymers were tested at 240°C in a Brabender Plasticorder with a 50 ml mixing head and standard rotors while the torque was recorded at 60 rev min^{-1}. Ternary blends were prepared by simultaneous extrusion of all components using a Killion single-screw extruder ($L/D = 30$, 2.54 cm diameter) at 240°C and a screw speed of 30 rev min^{-1}. The extruded pellets were injection moulded into standard tensile (ASTM D638 type I) and Izod (ASTM D256) bars (thickness = 0.3175 cm) using an Arburg screw injection moulding machine. Before each processing step, all materials containing polyamides were dried for at least 12 h at 85°C in a vacuum oven to ensure removal of sorbed water. All mechanical properties were determined for dry as-moulded specimens.

Transmission electron microscopy (TEM) was used to examine the blend morphology from sections cryogenically microtomed from Izod bars perpendicular to the flow direction. The butadiene rubber phase in the ABS was stained using osmium tetroxide (OsO_4) by exposing the ultra-thin microtomed samples to vapour from a 2% aqueous solution of OsO_4 for at least 8 h. Phosphotungstic acid (PTA) was used to stain the polyamide phase selectively[39-43]. This procedure involved floating the samples in a 2% aqueous solution of phosphotungstic acid for 30 min. In some cases, the two techniques were used simultaneously by first staining the samples with PTA and then exposing them to OsO_4 vapour for at least 8 h.

EFFECT OF POLYAMIDE MOLECULAR WEIGHT

Table 1 lists the mechanical properties of some of the polyamides used in this work. The nylon-6 and nylon-6,6 materials have very similar impact properties in spite of the variations in the molecular weight and their chemical differences. The tensile moduli of the nylon-6/nylon-6,6 copolymers, however, are slightly lower than those of the homopolyamides. The polyamides with higher CH_2/NHCO ratios (nylon-6,12, nylon-11 and nylon-12,12) also have significantly lower moduli and yield strengths and somewhat higher impact strengths. A series of nylon-11 materials with widely varying molecular weights all had mechanical properties similar to that observed for the BMNO TL material.

Table 2 also shows the mechanical properties of the ABS material (BL-65) and its 50/50 blend with the Capron 8207F nylon-6. This mixture exhibits mechanical

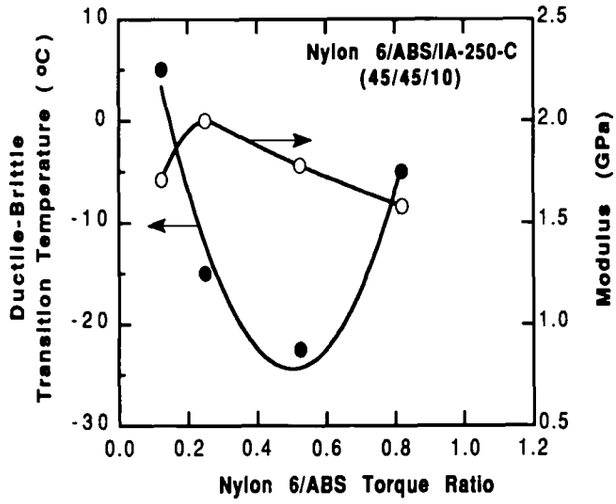

Figure 1 Effect of nylon-6/ABS torque ratio on the ductile–brittle transition temperature and tensile modulus of nylon-6/ABS (45/45) blends containing 10% IA-250-C

Table 2 Mechanical properties of compatibilized nylon/ABS blends

Polymer	Izod impact ($J\ m^{-1}$)	Ductile–brittle transition temperature (°C)	Modulus (GPa)	Yield stress (MPa)	Elongation at break (%)
ABS (BL-65)	300	n.t.[a]	0.8	17	98
Nylon-6 (8207F)/ABS (BL-65) (50/50)	105	n.t.	1.5	34	50
IA-250-C	20	n.t.	3.5	89	5
Nylon-6 (8202)/ABS/IA-250-C (45/45/10)	915	5	1.7	n.t.	n.t.
Nylon-6 (8207F)/ABS/IA-250-C (45/45/10)	970	−15	2.0	42	145
Nylon-6 (8209)/ABS/IA-250-C (45/45/10)	958	−23	1.8	n.t.	n.t.
Nylon-6 (B5)/ABS/IA-250-C (45/45/10)	1090	−5	1.6	44	115
Nylon-11 (BMNO TL)/ABS/IA-250-C (45/45/10)	585	5	1.1	n.t.	n.t.
Nylon-11 (BESNO TL)/ABS/IA-250-C (45/45/10)	676	−43	1.0	n.t.	n.t.
Nylon-11 (BESVO)/ABS/IA-250-C (45/45/10)	654	−35	1.0	n.t.	n.t.
Nylon-11 (BESHVO)/ABS/IA-250-C (45/45/10)	690	−35	1.0	n.t.	n.t.
Nylon-6,6/ABS/IA-250-C (45/45/10)	150	65	1.9	40	n.t.
Vydyne 86X/ABS/IA-250-C (45/45/10)	850	12	1.5	38	n.t.
XPN 1539F/ABS/IA-250-C (45/45/10)	1070	−18	1.5	36	n.t.
XPN 1250/ABS/IA-250-C (45/45/10)	950	−5	1.7	41	n.t.

[a] n.t. = not tested

properties that lie approximately on or slightly below the tie line connecting the properties of the two phases. Similar blends based on the other polyamides shown in *Table 1* exhibit analogous properties. It is clear that the IA-250-C compatibilizer is very brittle.

Nylon-6-based blends

For this comparison, a series of nylon-6 materials was selected that differ only in their molecular weight, which is reflected in the melt viscosities of these materials as measured by Brabender torque rheometry (see *Table 1*). *Table 2* shows the mechanical properties of blends of these nylon-6 materials with ABS at a 45/45 ratio containing 10% IA-250-C compatibilizer. All of the nylon-6 materials in this series led to super-tough blends at room temperature (*Table 2*). *Figure 1* shows the ductile–brittle transition temperature and tensile modulus of these blends as a function of the melt viscosity ratio of the two pure major phases. There is a minimum in the ductile–brittle transition temperature at a melt viscosity ratio near about 0.5, corresponding to Capron 8209, while the tensile modulus shows a slight maximum at a lower viscosity ratio, corresponding to Capron 8207F.

Figure 2 shows TEM photomicrographs for blends in this series stained by different techniques. Capron 8202 has the lowest melt viscosity in this series, and its blends have large ABS domains (see *Figures 2a* and *2b*). The ABS domain size can be deduced from specimens stained with OsO_4 (*Figure 2a*); however, this is more clear using the phosphotungstic acid (PTA) staining technique, since it precisely defines the nylon-6/ABS boundaries (*Figure 2b*). *Figure 2c* shows the photomicrograph for the blend based on Capron 8207F stained with PTA. The ABS domains appear to be more efficiently dispersed. *Figures 2d* and *2e* show photomicrographs for blends based on Capron 8209. For the OsO_4-stained blend (*Figure 2d*), the ABS domains appear to be aligned in elongated structures, and this becomes more evident using the PTA staining technique (*Figure 2e*). Through the latter staining technique, clear evidence for co-continuous character of the ABS phase also emerges. *Figures 2f* and *2g* show photomicrographs for blends based on B5 nylon-6. Both staining techniques clearly reveal co-continuous structures for this blend. For the blend stained with both PTA and OsO_4, the butadiene rubber particles inside the ABS domains can be clearly observed.

One can attribute the differences in the morphology of these blends to the variation in rheological properties of the polyamide phase, since their chemical characteristics are similar. Although Brabender torque rheometry only provides a rough characterization of the true melt viscosities prevailing inside the extruder, it is possible to draw some useful conclusions from these data. The large ABS domains observed in the case of the Capron 8202

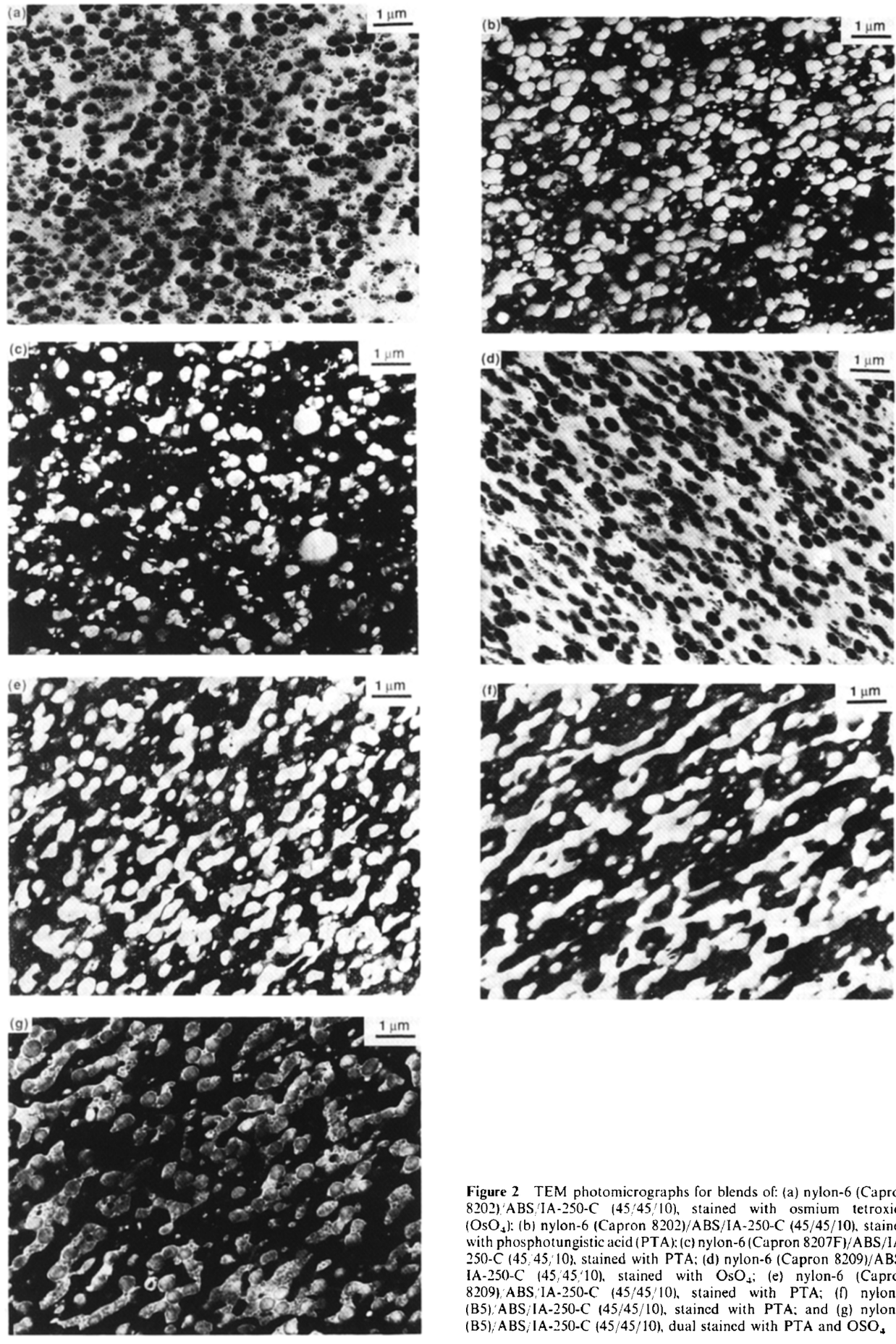

Figure 2 TEM photomicrographs for blends of: (a) nylon-6 (Capron 8202)/ABS/IA-250-C (45/45/10), stained with osmium tetroxide (OsO_4); (b) nylon-6 (Capron 8202)/ABS/IA-250-C (45/45/10), stained with phosphotungistic acid (PTA); (c) nylon-6 (Capron 8207F)/ABS/IA-250-C (45/45/10), stained with PTA; (d) nylon-6 (Capron 8209)/ABS/IA-250-C (45/45/10), stained with OsO_4; (e) nylon-6 (Capron 8209)/ABS/IA-250-C (45/45/10), stained with PTA; (f) nylon-6 (B5)/ABS/IA-250-C (45/45/10), stained with PTA; and (g) nylon-6 (B5)/ABS/IA-250-C (45/45/10), dual stained with PTA and OSO_4

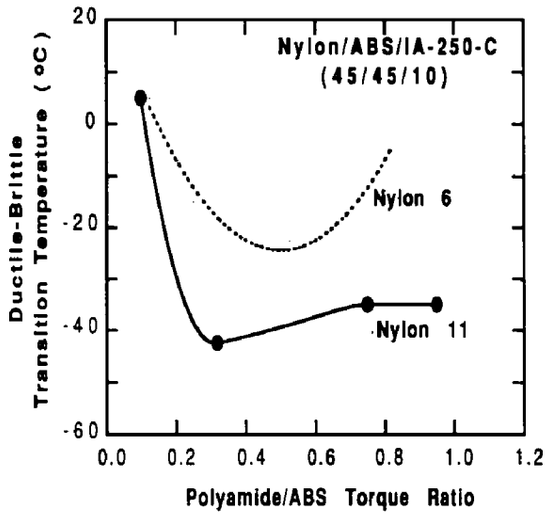

Figure 3 Effect of nylon-11/ABS torque ratio on the ductile–brittle transition temperature of nylon-11/ABS (45/45) blends containing 10% IA-250-C. The dotted curve represents the ductile–brittle transition temperatures of nylon-6 blends from *Figure 1*

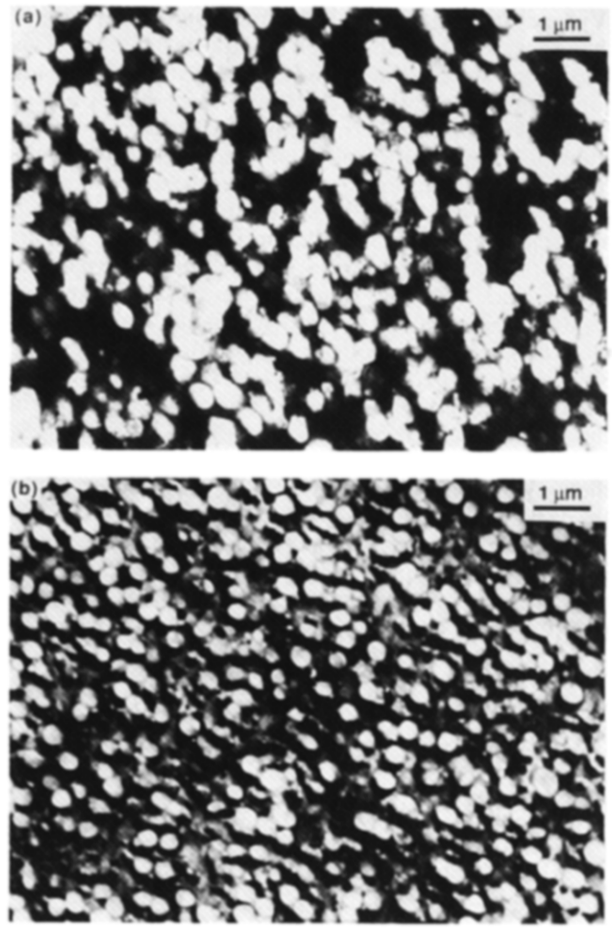

Figure 4 TEM photomicrographs for blends of (a) nylon-11 (BMNO TL)/ABS/IA-250-C (45/45/10) and (b) nylon-11 (BESHVO)/ABS/IA-250-C (45/45/10). The polyamide phase in both these blends was stained with PTA

nylon-6 blend are, no doubt, a result of the large mismatch in melt viscosities of the two phases[44–46]. The relatively poor mechanical properties (see *Table 2*) obtained for this blend could be a direct result of the inefficient dispersion of the ABS domains observed in *Figures 2a* and *2b*. The Capron 8207F blend shows the best dispersion of the ABS phase, a low value for the ductile–brittle transition temperature, and the maximum tensile modulus in this series. The Capron 8209 nylon-6 blend has the lowest ductile–brittle transition temperature in this series but a lower tensile modulus than the corresponding 8207F blend. It is likely that the elongated, almost co-continuous character of the relatively soft ABS domains in this case is responsible for the low tensile modulus of this blend. There is an even greater degree of co-continuity for the B5 blend (*Figures 2f* and *2g*), and an abrupt rise in the ductile–brittle transition temperature accompanied by a further reduction in the tensile modulus.

Nylon-11-based blends

Table 2 shows the mechanical properties of blends based on a series of nylon-11 materials of varying molecular weights and viscosity. Each of these blends is super-tough at room temperature, although their ductile–brittle transition temperatures show some variation with the melt viscosity of the polyamide phase (*Figure 3*). The blend based on the nylon-11 with the lowest molecular weight or viscosity shows relatively poor low-temperature impact properties, while the other blends in this series have more similar ductile–brittle transition temperatures. The tensile modulus remains more or less constant for this series of blends (*Table 2*). The lower ductile–brittle transition temperatures of nylon-11-based blends compared to those based on nylon-6 (see dotted curve in *Figure 3*) can be attributed to the more ductile character of the nylon-11 matrix resulting from its higher CH_2/NHCO ratio in the repeat unit[35].

TEM photomicrographs for two of the nylon-11 blends are shown in *Figure 4* where the polyamide phase has been stained with phosphotungstic acid. The blend based on nylon-11 with the lowest melt viscosity (BMNO TL), and thus the greatest viscosity mismatch with the ABS phase, shows large ABS domains (*Figure 4a*), which is probably the cause of the poor low-temperature properties observed. The ABS phase is more efficiently dispersed in the blend based on the highest-molecular-weight nylon-11 (BESHVO) (see *Figure 4b*); however, there is some tendency towards elongated ABS structures.

EFFECT OF CHEMICAL CHARACTERISTICS OF THE POLYAMIDE MATRIX

This section explores the effects of having two amine end-groups per polyamide chain and varying the CH_2/NHCO ratio in the repeat unit of these difunctional (nylon-*x*,*y*) polyamides on the morphology and mechanical properties of their compatibilized blends with ABS.

Nylon-6/nylon-6,6 copolymer-based blends

Table 2 shows the mechanical properties of the copolyamide/ABS blends where the nylon-6/nylon-6,6 ratio is varied. All blends, except those based on pure nylon-6,6 are super-tough at room temperature. The tensile properties of the blends based on the copolymer

(Vydyne 86X and XPN 1539F) are somewhat poorer than those for blends based on nylon-6 or nylon-6,6. This is expected since the modulus and yield strength of these copolymers are lower than those of either nylon-6 or nylon-6,6 (*Table 1*). *Figure 5* shows how the ductile–brittle transition temperature of these blends changes as the nylon-6 content in the copolyamide phase is increased. Vydyne 86X, which contains only 16% nylon-6, leads to a dramatically lower ductile–brittle transition than is seen for the corresponding blend based on nylon-6,6. The lowest ductile–brittle transition temperatures in this series are obtained for the pure nylon-6 (Capron 8207F) material and the copolymer, XPN 1539F, containing 85% nylon-6. The dotted curve in *Figure 5* shows the dispersed-phase particle size for compatibilized blends of the polyamide with SAN 25 determined earlier[21]. The variation in the ductile–brittle transition temperatures of these nylon/ABS blends parallels the trend observed for the dispersed-phase particle size for nylon/SAN systems[21]. The larger particle size in the difunctional polyamide blends was attributed to the difficulty in breaking down dispersed particles when there is two-point chemical grafting that is possible with the nylon-*x*,*y* materials

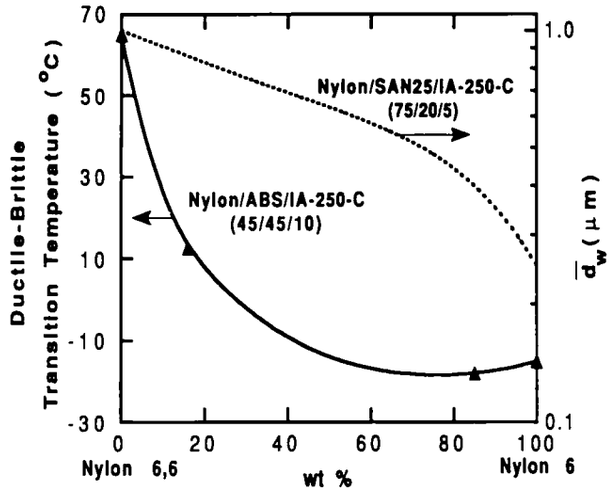

Figure 5 Effect of nylon-6,6 content of polyamide copolymers on the ductile–brittle transition temperature of nylon/ABS/IA-250-C (45/45/10) blends. The dotted curve shows the dispersed-phase particle size *versus* nylon-6,6 content in copolyamide blends of nylon/SAN 25/IA-250-C (75/20/5) from ref. 21

where a certain fraction of the chains have two amine end-groups.

Figure 6 shows TEM photomicrographs for the series of blends whose properties are shown in *Figure 5*. The nylon-6,6-based blend (see *Figures 6a* and *6b*) has large ABS domains, which probably contribute to the brittle nature of this blend. The photomicrographs for the blend based on Vydyne 86X copolymer (*Figures 6c* and *6d*) also show large ABS domains. The XPN 1539F-based blend has smaller ABS domains than do blends based on nylon-6,6 or the Vydyne 86X material; however, the domains are distinctly larger than those observed for the Capron 8207F-based blend (*Figure 2c*).

It does not seem possible to rationalize the dramatic changes in the ductile–brittle transition temperatures of these blends solely on the basis of their morphology. For example, the nylon-6,6 and Vydyne 86X blends have almost the same level of dispersion of the ABS phase, but the ductile–brittle transition temperature for the Vydyne 86X-based blend is almost 50°C lower than that observed for the corresponding blend with nylon-6,6. The blends formed from the copolymer XPN 1539F show significantly larger ABS domains than are seen in the Capron 8207F-based blends; however, the blends formed from the copolymer have a distinctly lower ductile–brittle transition temperature. These observations suggest that the inherent ductility of the polyamide matrix also plays an important role in determining the ductile–brittle transition temperature in addition to morphology. The enhanced inherent ductility and the lower values for the tensile modulus for both the pure copolymer polyamides (Vydyne 86X and XPN 1539F) and their blends (see *Tables 1* and *2*) no doubt stem from the lower crystallinity of these copolymers.

Table 3 compares heat-of-fusion data for the pure polyamides in this series and for their blends. The heat of fusion was computed by integrating the melting-peak area in the d.s.c. scan using consistent integration limits. The heat of fusion for the first heat (ΔH_1) characterizes the state of the moulded specimen and is expected to be somewhat influenced by the thermal and mechanical history imposed by the moulding operation; whereas the values from the second heat (ΔH_2) should be free of this particular history. The latter should allow comparison of the materials against a standard thermal history imposed by the d.s.c. protocol. It is clear from *Table 3* that the heat of fusion and hence the crystallinity are much lower for the two copolyamides than for the

Table 3 Crystallinity of compatibilized nylon/ABS blends

		Heats of fusion for pure polyamide[a,b]		Heats of fusion for polyamide/BL-65/IA-250-C (45/45/10) blend[a,b]			
Polyamide	T_m (°C)	ΔH_1 (first heat)	ΔH_2 (second heat)	ΔH_{1b} (first heat)	ΔH_{2b} (second heat)	$\Delta H_{1b}/\Delta H_1$	$\Delta H_{2b}/\Delta H_2$
Nylon-6 (8207F)	220	55.0	80.1	27.6	32.1	0.49	0.40
XPN 1539F	200	45.9	49.2	19.6	20.5	0.42	0.41
Vydyne 86X	233	47.5	66.0	27.4	27.7	0.57	0.42
Nylon-6,6	261	60.0	82.6	41.5	38.4	0.69	0.46

[a]Integration limits for computing melting-peak area for neat polyamides and blends of nylon-6 (8207F) and XPN 1539F are 130–240°C while for Vydyne 86X and nylon-6,6 the limits are 145–275°C
[b]Scan rate of 20°C min^{-1} for both heating/cooling

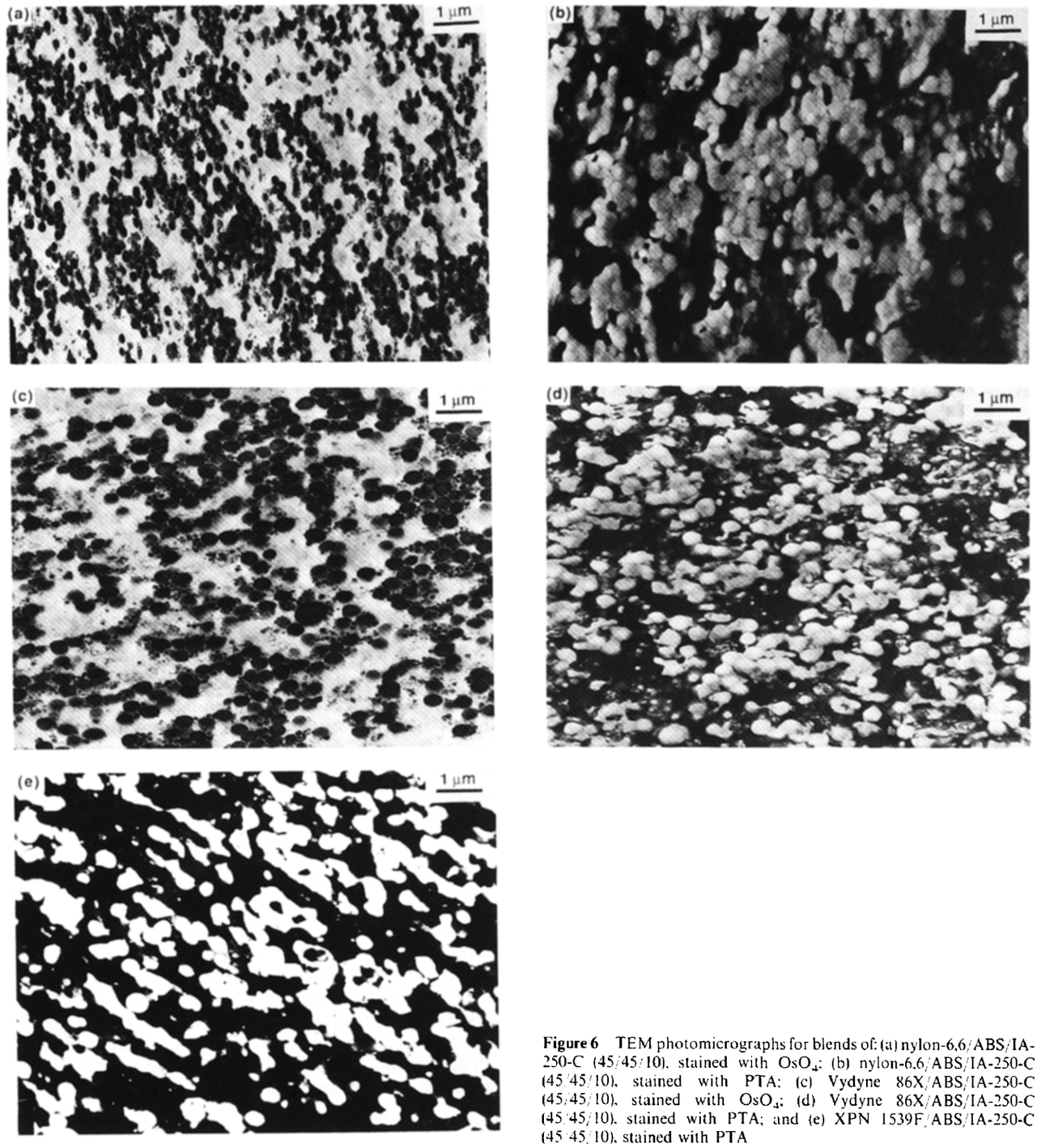

Figure 6 TEM photomicrographs for blends of: (a) nylon-6,6/ABS/IA-250-C (45/45/10), stained with OsO_4; (b) nylon-6,6/ABS/IA-250-C (45/45/10), stained with PTA; (c) Vydyne 86X/ABS/IA-250-C (45/45/10), stained with OsO_4; (d) Vydyne 86X/ABS/IA-250-C (45/45/10), stained with PTA; and (e) XPN 1539F/ABS/IA-250-C (45/45/10), stained with PTA

homopolyamides. In the case of aliphatic polyamides, lower crystallinity translates into greater ductility. We believe that this effect is largely responsible for the much lower ductile–brittle transition temperature for the Vydyne 86X blend compared to the nylon-6,6 blend; both blends have very similar phase morphologies. This would also explain the slightly lower ductile–brittle transition temperature for the XPN 1539F blend compared to that for the Capron 8207F blend, where the former actually has significantly poorer ABS dispersion.

One might expect some changes in the crystallinity of the polyamide phase resulting from the blending process[47–49] and the associated chemical reaction[50]. A measure of the degree of crystallinity in these blends can be obtained by dividing the absolute value of the d.s.c. peak area for the compatibilized blend by the corresponding value for the pure polyamide material as shown in *Table 3*. This ratio should be 0.45 if the factors involved in processing do not change the crystallinity of the polyamide in the blend. In these computations, the second heat of fusion is considered to be more independent of the processing conditions and forms the basis for these conclusions. The ratios for three of the blends shown in *Table 3* are slighly lower than 0.45, signifying lower levels

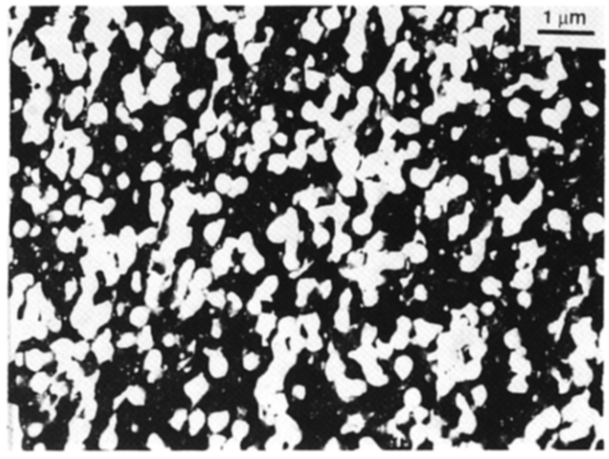

Figure 7 TEM photomicrograph of XPN 1250/ABS/IA-250-C (45/45/10) blend. The polyamide phase was stained with PTA

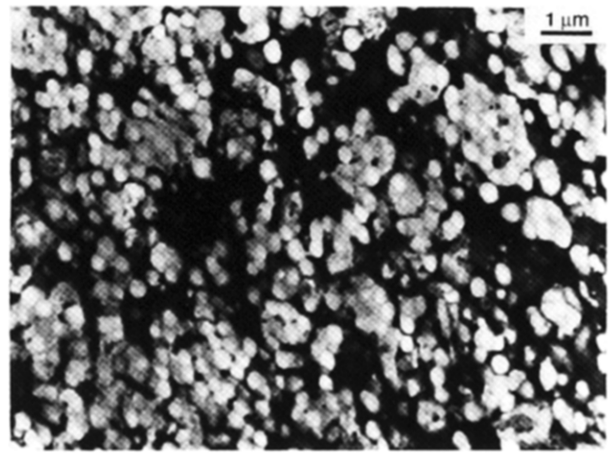

Figure 9 TEM photomicrograph of nylon-6,10/ABS/IA-250-C (45/45/10) blend. The polyamide phase was stained with PTA

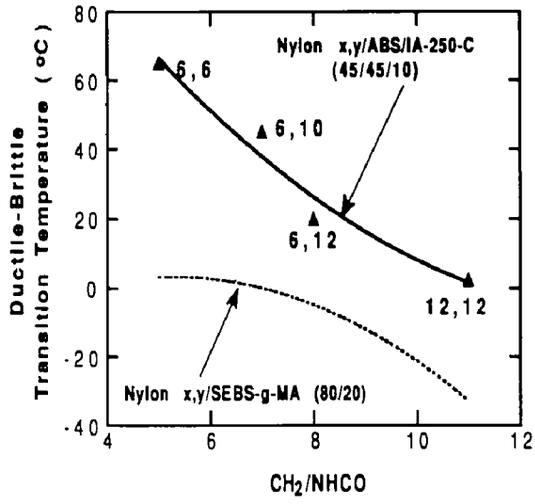

Figure 8 Ductile–brittle transition temperature as a function of polyamide CH_2 NHCO ratio for nylon-*x,y*/ABS/IA-250-C blends. The dotted curve represents the ductile–brittle transition temperatures of nylon-*x,y* SEBS-*g*-MA (80 20) blends from ref. 35

of crystallinity of the polyamide phase in these blends than observed in the corresponding neat polyamides. Martuscelli *et al.* suggested that grafting of an elastomeric phase to a polyamide material reduces the rate of nylon crystallization and, therefore, the crystallinity achieved in the blend for a fixed crystallization protocol[50].

Figure 7 shows the morphology of a blend based on the XPN 1250 nylon-6 material. Although, the ABS appears to be quite efficiently dispersed in this case, some relatively large, elongated domains are observed. This particular nylon-6 has a significantly greater number of amine end-groups than carboxyl ends, which leads to a population of relatively large, complex particles in the model nylon/SAN system as shown previously[21]. As seen in *Table 2*, its blend with ABS is super-tough at room temperature but has a higher ductile–brittle transition temperature than the corresponding Capron 8207F blend (see *Table 2*). We believe that this is a direct consequence of the less efficiently dispersed ABS domains caused by the difunctional character of this nylon matrix, since both polyamides (8207F and XPN 1250) have similar inherent ductilities and melt viscosities (see *Table 1*).

Effect of CH_2/NHCO ratio for nylon-x,y-based blends

Figure 8 shows the ductile–brittle transition temperature for compatibilized blends of ABS with a series of difunctional nylon-*x,y* materials that span a wide range of CH_2/NHCO ratios. All of the blends in this series have relatively large ABS domains similar to that observed in the case of nylon-6,6. Blends based on nylon-6,10 are brittle at room temperature and have quite large ABS domains (see *Figure 9*). The trend in the ductile–brittle transition temperature for this series of blends seems to relate strongly to the inherent ductility of the polyamide matrix as the CH_2/NHCO ratio is varied. This hypothesis is further strengthened by the relatively small variations in the blend morphology observed in this series (see *Figures 6a, 6b* and *9*). The dotted curve in *Figure 8* shows the variation in the ductile–brittle transition temperature for blends of these same polyamides with SEBS-*g*-MA as reported in our earlier work[35]. The ductile–brittle transition temperatures for the compatibilized nylon-*x,y*/ABS blends are distinctly higher than those for the blend with SEBS-*g*-MA. Probable reasons for this may lie in differences in the structure and nature of the rubber-containing phase in addition to morphological issues.

CONCLUSIONS

The effects of various physical and chemical characteristics of the polyamide components on the morphology and mechanical properties of reactively compatibilized nylon/ABS blends have been examined. In general, for a fixed composition and compatibilizing polymer (IA-250-C), the best combination of mechanical properties (tensile and impact) results from the most efficient dispersion of the ABS domains in the polyamide matrix. For nylon-6, there is a relatively narrow range of polyamide-phase melt viscosities relative to the ABS within which the most optimum combination of mechanical properties was observed (*Figure 1*). For nylon-11, on the other hand, this range is significantly broader, as evident in *Figure 3*.

For blends of difunctional polyamides (e.g. nylon-*x*,*y*, copolymers of nylon-6/nylon-6,6 and nylon-6 enriched in amine end-groups), it is more difficult to achieve efficient dispersion of the ABS phase. This has been attributed to the two-point grafting mechanism possible in these polyamides, which have a fraction of chains with two amine ends that can react with the acid functionality of the imidized acrylic compatibilizer.

Blend toughness is more easily achieved the greater the inherent ductility of the polyamide phase. The inherent ductility of the polyamide matrix was increased here via a lower crystallinity, e.g. copolymers of nylon-6/nylon-6,6, or higher CH_2/NHCO ratio in the repeat units (*Figures 5* and *8*).

ACKNOWLEDGEMENTS

This research was supported by the US Army Research Office. The authors are indebted to Rohm and Haas Co. for supplying the various imidized acrylic compatibilizers used in this work. The authors are grateful to A. J. Oshinski for the polyamide end-group analysis data and to Mr Daniel Kallick of the Photography Department at the University of Texas at Austin.

REFERENCES

1 Xanthos, M. *Polym. Eng. Sci.* 1988, **18**, 1392
2 Baker, W. E. and Saleem, M. *Polymer* 1987, **28**, 2057
3 Wu, S. *Polymer* 1985, **26**, 1855
4 Hobbs, S. Y., Bopp, R. C. and Watkins, V. H. *Polym. Eng. Sci.* 1983, **23**, 380
5 Liu, N. C. and Baker, W. E. *Adv. Polym. Technol.* 1992, **11**, 249
6 Borggreve, R. J. M. and Gaymans, R. J. *Polymer* 1989, **30**, 63
7 Borggreve, R. J. M., Gaymans, R. J. and Schuijer, J. *Polymer* 1989, **30**, 71
8 Borggreve, R. J. M., Gaymans, R. J. and Luttmer, A. R. *Makromol. Chem., Macromol. Symp.* 1988, **16**, 195
9 Lavengood, R. E. and Silver, F. M. *SPE Tech. Papers* 1987, **33**, 1369
10 Lavengood, R. E., Padwa, A. R. and Harris, A. F. US Pat. 4713415, 1987 (assigned to Monsanto)
11 Lavengood, R. E., Patel, R. and Padwa, A. R. US Pat. 4777211, 1988 (assigned to Monsanto)
12 Howe, D. V. and Wolkowicz, M. D. *Polym. Eng. Sci.* 1987, **27**, 1582
13 Howe, D. V. and Wolkowicz, M. D. *SPE Techn. Papers* 1986, **32**, 324
14 Aoki, Y. and Watanabe, M. US Pat. 4987185, 1991 (assigned to Monsanto Kasei Co.)
15 Padwa, A. R. and Lavengood, R. E. *ACS Symp. Ser.* 1992, **33**, 600
16 Paul, D. R. in 'Advances in Polymer Blends and Alloys Technology' (Ed. K. Finlayson), Technomic, Lancaster, PA, 1993, Vol. 4, p. 80
17 Angola, J. C., Fujita, Y., Sakai, T. and Inoue, T. *J. Polym. Sci., Polym. Phys. Edn.* 1988, **26**, 807
18 Aoki, Y. and Watanabe, M. *Polym. Eng. Sci.* 1992, **32**, 878
19 Triacca, V. J., Ziaee, S., Barlow, J. W., Keskkula, H. and Paul, D. R. *Polymer* 1991, **32**, 1401
20 Takeda, Y. and Paul, D. R. *J. Polym. Sci. (B) Polym. Phys.* 1992, **30**, 1273
21 Majumdar, B., Keskkula, H., Paul, D. R. and Harvey, N. G. *Polymer* 1994, **35**, 4263
22 Majumdar, B., Keskkula, H. and Paul, D. R. *Polymer* 1994, **35**, 5453
23 Buskirk, B. and Akkapeddi, M. K. Proc. IUPAC 33rd Int. Symp. on Macromolecules, Session 3.2.3, Montreal, 1990
24 Hallden-Abberton, M. US Pat. 4246374, 1989 (to Rohm and Haas)
25 Hallden-Abberton, M. *Polym. Mater. Sci. Eng.* 1991, **65**, 361
26 Hallden-Abberton, M., Cohen, L. and Wood, R. US Pat. 4874824, 1989 (to Rohm and Haas)
27 Hallden-Abberton, M., Bortnick, N., Cohen, L., Freed, W. and Fromuth, H. US Pat. 4727117, 1988 (to Rohm and Haas)
28 Fowler, M. E., Paul, D. R., Cohen, L. A. and Freed, W. T. *J. Appl. Polym. Sci.* 1989, **37**, 513
29 Work, J. L. *Polym. Eng. Sci.* 1973, **13**, 52
30 Avgeropoulos, G. N., Weissert, F. C., Biddison, P. H. and Bohm, G. G. A. *Rubber Chem. Technol.* 1975, **49**, 93
31 Paul, D. R. and Barlow, J. W. *J. Macromol. Sci.–Rev. Macromol. Chem. (C)* 1980, **18**, 109
32 Jordhamo, G. M., Manson, J. A. and Sperling, L. H. *Polym. Eng. Sci.* 1986, **26**, 517
33 Oshinski, A. J., Keskkula, H. and Paul, D. R. *Polymer* 1992, **33**, 268 and 284
34 Takeda, Y., Keskkula, H. and Paul, D. R. *Polymer* 1992, **33**, 3173
35 Majumdar, B., Keskkula, H. and Paul, D. R. *Polymer* 1994, **35**, 1386, 1399
36 Oshinski, A. J. University of Texas, personal communication, 1993
37 Kim, H., Keskkula, H. and Paul, D. R. *Polymer* 1990, **31**, 869
38 Kim, J. H., Keskkula, H. and Paul, D. R. *J. Appl. Polym. Sci.* 1990, **40**, 183
39 Martinez-Salazar, J. and Cannon, C. G. *J. Mater. Sci. Lett.* 1984, **3**, 693
40 Morel, D. E. and Grubb, D. T. *Polymer* 1984, **25**, 41
41 Boylston, E. K. and Rollins, M. L. *Microscope* 1971, **19**, 255
42 Spit, B. J. *Faserforsch. Textiltech.* 1967, **18**, 161
43 Rusnock, J. A. and Hansen, D. *J. Polym. Sci. (A)* 1965, **3**, 617
44 Wu, S. *Polym. Eng. Sci.* 1987, **27**, 335
45 Serpe, G., Jarrin, J. and Dawans, F. *Polym. Eng. Sci.* 1990, **30**, 553
46 Favis, B. D. and Chalifoux, J. P. *Polym. Eng. Sci.* 1987, **27**, 1591
47 Karger-Kocsis, J., Kallo, A., Szafner, A., Bodor, G. and Senyei, Z. *Polymer* 1979, **20**, 37
48 Karger-Kocsis, J. and Kulezhev, V. N. *Polymer* 1982, **23**, 699
49 Ramsteiner, F., Kanig, G., Heckman, W. and Gruber, W. *Polymer* 1983, **24**, 365
50 Martuscelli, E., Riva, F., Sellitii, C. and Silvestre, C. *Polymer* 1985, **26**, 270